Possible involvement of innate immune cells expressing the macrophage galactose-type C-type lectin in inflammatory skin diseases

Hahn JM, McFarland KL, Combs KA, Anness MC, Supp DM. Analysis of HOX gene expression and the effects of HOXA9 overexpression in fibroblasts derived from keloid lesions and normal skin. Wound Repair Regen 2021;29:777–91.

Martincorena I, Roshan A, Gerstung M, Ellis P, Van Loo P, McLaren S, et al. Tumor evolution. High burden and pervasive positive selection of somatic mutations in normal human skin. Science 2015;348:880–6.

Muse ME, Bergman DT, Salas LA, Tom LN, Tan JM, Laino A, et al. Genome-scale DNA methylation analysis identifies repeat element alterations that modulate the genomic stability of melanocytic nevi. J Invest Dermatol 2022;142:1893–1902.e7.

Nakamura T, Gehrke AR, Lemberg J, Szymaszek J, Shubin NH. Digits and fin rays share common developmental histories. Nature 2016;537:225–8.

Philippidou P, Dasen JS. Hox genes: choreographers in neural development, architects of circuit organization. Neuron 2013;80:12–34.

Rinn JL, Wang JK, Allen N, Brugmann SA, Mikels AJ, Liu H, et al. A dermal HOX transcriptional program regulates site-specific epidermal fate. Genes Dev 2008;22:303–7.

Rosendahl C, Marozava A. Dermatoscopy and skin cancer: a handbook for hunters of skin cancer and melanoma. 1st ed. Scion Publishing; 2019. p. 384.

Stark MS, Tan JM, Tom L, Jagirdar K, Lambie D, Schaider H, et al. Whole-exome sequencing of acquired nevi identifies mechanisms for development and maintenance of benign neoplasms. J Invest Dermatol 2018;138:1636–44.

Tan JM, Tom LN, Jagirdar K, Lambie D, Schaider H, Sturm RA, et al. The BRAF and NRAS mutation prevalence in dermoscopic subtypes of acquired naevi reveals constitutive mitogen-activated protein kinase pathway activation. Br J Dermatol 2018;178:191–7.

Weiss JM, Hunter MV, Cruz NM, Baggiolini A, Tagore M, Ma Y, et al. Anatomic position determines oncogenic specificity in melanoma. Nature 2022;604:354–61.

Possible Involvement of Antigen-Presenting Cells Expressing the Macrophage Galactose-Type C-Type Lectin in Inflammatory Skin Diseases

JID Open

Journal of Investigative Dermatology (2023) **143,** 1834–1838; doi:10.1016/j.jid.2023.03.1654

TO THE EDITOR

Atopic dermatitis (AD) and psoriasis (Pso) are common systemic inflammatory skin diseases in which dendritic cells (DCs) and macrophages (MØs) play central roles. Clarifying the cell subsets that are involved in the pathogenesis of AD and Pso is a prerequisite to developing effective treatments. Our research focuses on macrophage galactose-type C-type lectin (MGL)/CLEC10A/CD301 (referred to as MGL in the remaining parts of this paper), which is expressed on limited subpopulations of DCs and MØs but not on Langerhans cells (Kumamoto et al., 2009; Murakami et al., 2013; Polak et al., 2014) and is involved in the initiation of antigen presentation and signal transduction (Denda-Nagai et al., 2010; Kanemaru et al., 2019; Kurashina et al., 2021). Mouse MGL2/CD301b is likely to be the orthologous protein of human MGL. $MGL2^+$ cells are involved in the skewing of the immune response toward T helper (Th) 2 in mice (Gao et al., 2013; Kumamoto et al., 2013; Murakami et al., 2013). In addition, $MGL2^+$ DCs were significantly increased in psoriatic mouse skin and produced high levels of IL-23, which is associated with the pathogenesis of Pso (Kim et al., 2018). Such immune modulatory involvement of MGL^+ cells is potentially conserved in humans. Recent reports have shown that MGL-positive human type 2 DCs (i.e., cDC2) express CD1c, CD14, and CD163 (Bourdely et al., 2020; Brown et al., 2019; Heger et al., 2018). In addition, it has been reported that MGL^+CD14^+cDC2s were increased in inflammation and were related to Th17 cell differentiation in Pso (Nakamizo et al., 2021). However, the distribution, phenotype, and function of MGL^+ cells in human skin remain largely unknown.

In this study, we used biopsy specimens to identify human MGL^+ cells in healthy (healthy controls [HCs], n = 12), AD (n = 11), and Pso (n = 16) skin. Subject characteristics are shown in Supplementary Table S1. Materials and Methods can be found in the Supplementary information. MGL^+ cells were observed in both normal and pathological skin, mainly in the upper dermis, especially around vessels (Supplementary Figure S1 and Figure 1a–c). In both AD and Pso, MGL^+ cells were observed in the epidermis and dermis (Figure 1b and c), whereas in HCs, MGL^+ cells were rare in the epidermis (Figure 1a). No staining was observed with a control antibody (Supplementary Figure S2a). Quantification of cell numbers showed that MGL^+ cell density was increased in AD and Pso compared with that in HCs (Figure 1d–f), suggesting that MGL^+ cells are recruited or that MGL expression is induced during inflammation. Supportive analysis of two publicly available datasets—GSE121212 and E-MTAB-8149—that investigated AD, Pso, and HC skin biopsy specimens revealed that the *MGL* mRNA expression level was significantly higher in AD than in HC and in Pso than in HC specimens (Supplementary Results and Supplementary Figure S3).

Next, we investigated the correlation of MGL^+ cells with clinical parameters, including TARC/CCL17, a Th2 chemokine involved in allergic inflammation (Saeki and Tamaki, 2006). In AD skin, the number of MGL^+ cells in the dermis positively correlated with serum TARC/CCL17 levels, serum IgE levels, and the number of $TARC^+$ cells in the dermis

Abbreviations: AD, atopic dermatitis; DC, dendritic cell; HC, healthy control; MGL, macrophage galactose-type C-type lectin; MØ, macrophage; Pso, psoriasis; Th, T helper

Accepted manuscript published online 22 March 2023; corrected proof published online 24 April 2023

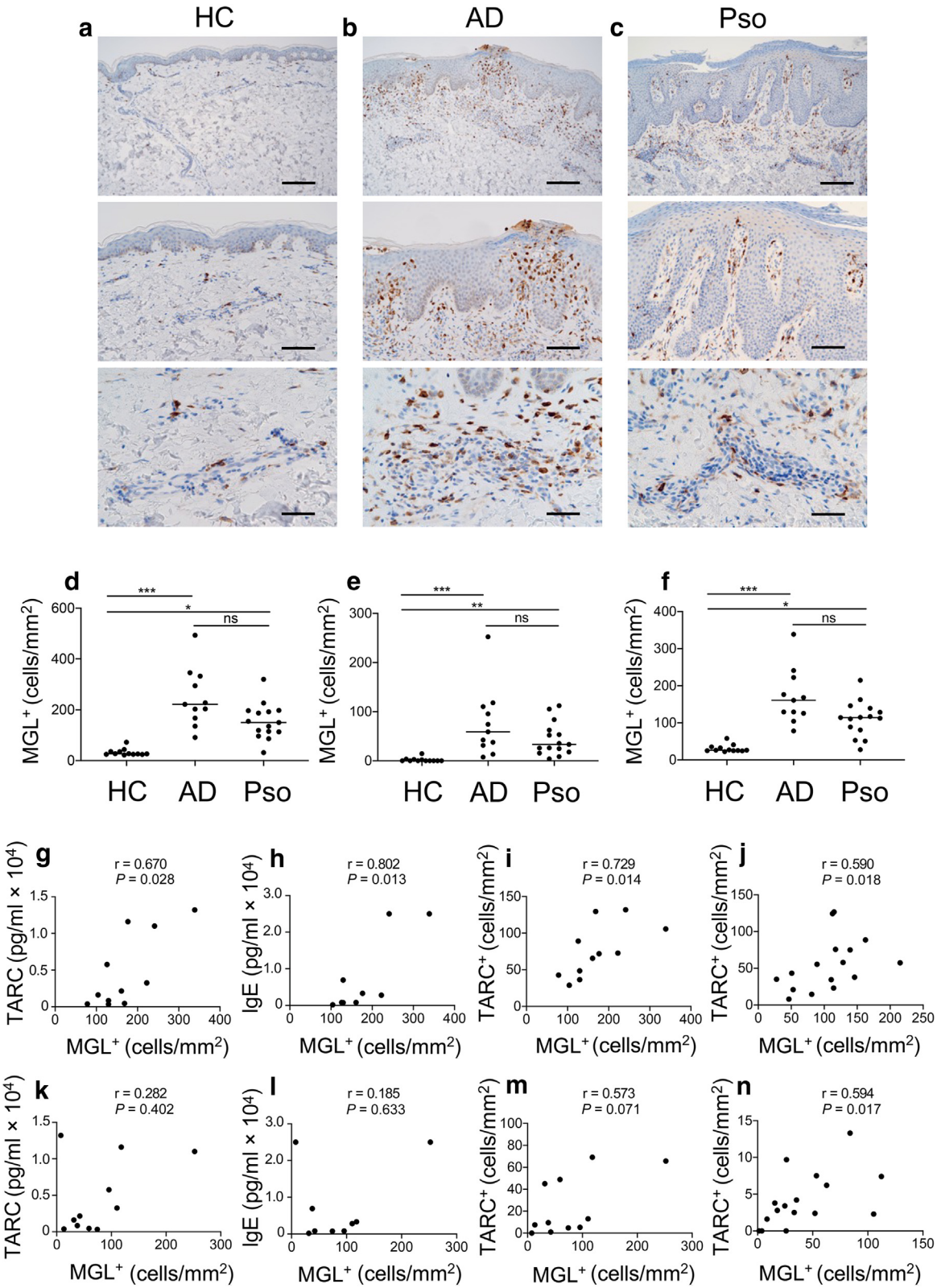

Figure 1. Distribution and density of MGL$^+$ cells in human skin and the correlation between the density of MGL$^+$ cells and clinical parameters. (**a**−**c**) MGL$^+$ cells in skin samples obtained from (**a**) HCs, (**b**) patients with AD, and (**c**) patients with Pso were immunohistochemically stained using a polyclonal antibody specific for MGL. Bars = 200 μm (for **a**−**c**, upper panel), 100 μm (for **a**−**c**, middle panel), and 50 μm (for **a**−**c**, bottom panel). (**d**−**f**) The numbers of MGL$^+$ cells per square millimeter were plotted for (**d**) the whole skin, (**e**) the epidermis, and (**f**) the upper dermis. One dot represents the cell count for an individual patient. The horizontal line represents the median. Analysis was performed with Kruskal−Wallis test. *** $P < 0.0001$, ** $P < 0.001$, and * $P < 0.05$. (**g**−**n**) The density of MGL$^+$ cells (**g**−**i**) in the AD dermis, (**k**−**m**) in the AD epidermis, (**j**) in the Pso dermis, and (**n**) in the Pso epidermis was compared with (**g, k**) serum TARC/CCL17 levels, (**h, l**) serum total IgE levels, and (**i, j, m, n**) the density of TARC$^+$ cells. Spearman's rank correlation r is shown. AD, atopic dermatitis; HC, healthy control; MGL, macrophage galactose-type C-type lectin; ns, not significant; Pso, psoriasis.

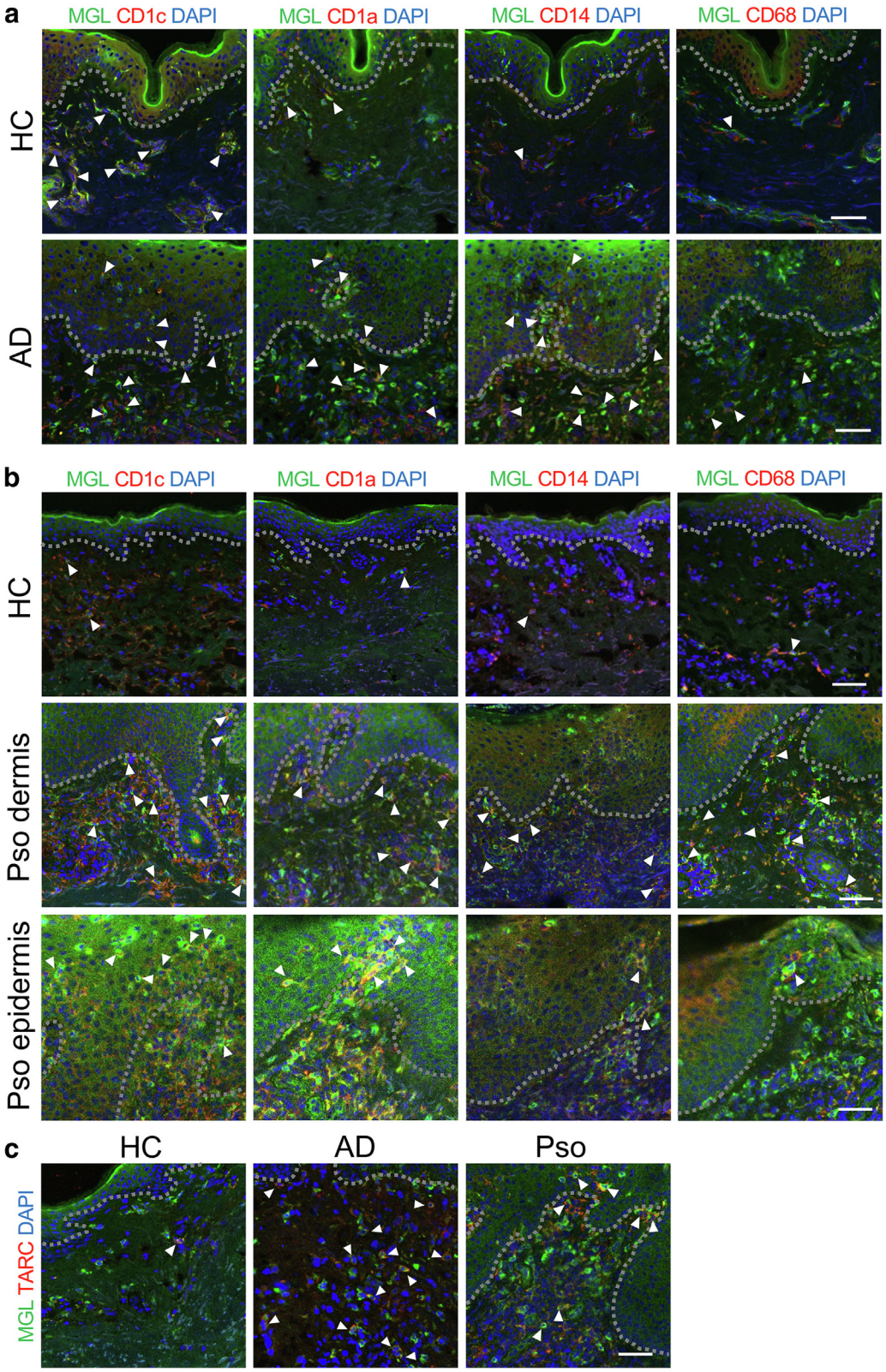

Figure 2. Phenotypes of MGL$^+$ cells in HC, AD, and Pso skin. (**a, b**) Biopsy specimens from HCs, patients with AD, and patients with Pso were costained with a mAb specific for MGL and antibodies specific for the innate immune cell markers CD1c, CD1a, CD14, and CD68. (**a**) AD skin and control; (**b**) Pso skin and control. The major double-stained population in HC, AD, and Pso skin was CD1c$^+$MGL$^+$ cells. (**c**) Biopsy specimens from HC, patients with AD, and patients with Pso were costained with a mAb specific for MGL and a polyclonal antibody specific for TARC/CCL17 and investigated by immunofluorescence. Specimens from three patients each were investigated, and representative images are shown. Arrowheads indicate double-stained cells. A thin, dotted line indicates the border between the dermis and the epidermis. Bar in (**a**) shows 50 μm. Bar in (**b**) shows 100 μm (upper and middle panel) and 50 μm (bottom panel). Bar in (**c**) shows 50 μm. AD, atopic dermatitis; HC, healthy control; MGL, macrophage galactose-type C-type lectin; Pso, psoriasis.

(Figure 1g–i). In the AD epidermis, no significant correlation with these markers was observed (Figure 1k–m). TARC/CCL17 serum levels correlated with the number of $TARC^+$ cells in the upper dermis but not in the epidermis (Supplementary Figure S4). There was no significant correlation between the Eczema Area and Severity Index and the number of MGL^+ cells (Supplementary Figure S2b and c). MGL^+ cells are not limited to a single-cell population, and patients with AD show some heterogeneity; for instance, some patients shift from a Th2 type to a Th1 type during the chronic cutaneous phase (Kataoka, 2014). Therefore, MGL^+ cell subsets should be investigated more systematically and in a larger number of subjects. Regarding Pso skin, the number of $TARC^+$ cells correlated with the number of MGL^+ cells in the epidermis and dermis (Figure 1j and n). The Psoriasis Area Severity Index did not correlate with the number of MGL^+ cells (Supplementary Figure S2d and e).

To characterize the subsets of MGL^+ DCs and MØs, we used antibodies specific for MGL and CD1c, CD1a, CD14, and CD68. The major double-stained cell populations in HC, AD, and Pso dermis were $CD1c^+MGL^+$ cells (Figure 2a and b and Supplementary Figure S5a and b). In AD and Pso, a few $CD1a^+MGL^+$, $CD14^+MGL^+$, and $CD68^+MGL^+$ cells were also observed in the upper dermis (Figure 2a and b and Supplementary Figure S5a and b). The percentage of MGL^+CD14^+ cells in the dermis was significantly higher in AD and Pso than in HC (Supplementary Figure S6). Previously, $CD1c^+$ DCs and $CD14^+$ MØs were reported in the steady state, and monocyte-derived DCs increased during inflammation (Kashem et al., 2017). Our data suggest that MGL expression is not limited to a single-cell subset but that MGL^+ cells are comprised of $CD1c^+$ DCs and a few $CD1a^+$ DCs and $CD14^+$DCs or MØs in the dermis of human skin.

In AD and Pso, $CD1c^+MGL^+$ cells were also observed in the epidermis, together with a few $CD1a^+MGL^+$ and $CD14^+MGL^+$ cells (Figure 2b, bottom panels, and Supplementary Figure S5b). This agrees with a previous report (Guttman-Yassky et al., 2007). Furthermore, in 9 of 11 AD specimens, a total of 14 spongiotic areas in the epidermis were found to be infiltrated by MGL^+ cells, similar to those shown in Figure 1b. Recent reports show that inflammatory dendritic epidermal cells accumulate in and Langerhans cells surround spongiotic areas in skin lesions of patients with AD (Tanei and Hasegawa, 2022, 2021). Therefore, it is plausible that MGL^+ cells might be involved in the formation and/or exacerbation or the suppression of spongiotic lesions as Langerhans cell–like cells or inflammatory dendritic epidermal cells.

Next, we stained HC, AD, and Pso patient skin sections with antibodies specific for MGL and TARC/CCL17 and counted the number of MGL^+TARC^+ double-positive cells. AD and Pso specimens contained significantly more MGL^+ cells, which were costained with TARC/CCL17, than HC specimens (Figure 2c and Supplementary Figures S5c and S6). In particular, 65.7% of MGL^+ cells in the AD dermis were costained with TARC/CCL17. In Pso, 42.3% of MGL^+ cells in the epidermis and 28.6% of MGL^+ cells in the dermis were costained with TARC/CCL17. The prevalence of MGL^+ cells among $TARC^+$ cells was 59.0% in the AD dermis and 66.7% in the Pso dermis. These findings suggest that a portion of MGL^+ cells coexpress TARC/CCL17 in both AD and Pso. Although Pso is regarded as a Th17-dominant disease, recent reports have shown that TARC/CCL17 levels are increased in subsets of patients with Pso, such as patients with severe pruritus (Nattkemper et al., 2018; Purzycka-Bohdan et al., 2022).

In conclusion, MGL^+ cells are present in healthy skin dermis but are sparse in the epidermis, and they significantly increase in AD and Pso lesions, where they are present in both the epidermis and dermis and infiltrate spongiotic areas in AD skin lesions. Both DCs and MØs are likely to express MGL, with $CD1c^+MGL^+$ DCs being the most prominent. In addition, a subset of MGL^+ cells in AD and Pso coexpress TARC/CCL17. Taken together, these findings encourage further exploration of the potential involvement of MGL^+ cells in inflammatory skin diseases, including the possibility that MGL could serve as a therapeutic target.

Ethics Statement

The study was approved by St. Luke's International Hospital Ethics Committee (approval number R-1502) and conducted in accordance with the Declaration of Helsinki Principles. Written informed consent for participation in the study and publication of the results was obtained from all patients included in the study.

Data availability statement

All data are contained within this article and its Supplementary information files.

ORCIDs

Yukari Manome-Zenke: http://orcid.org/0000-0002-5352-6511
Kaori Denda-Nagai: http://orcid.org/0000-0001-8325-3289
Miki Noji: http://orcid.org/0000-0002-9768-8969
Naoto Tsuneda: http://orcid.org/0000-0002-5758-3855
Katrin Beate Ishii-Schrade: http://orcid.org/0000-0002-9167-8831
Ryuichi Murakami: http://orcid.org/0000-0001-8257-585X
Naoki Kanomata: http://orcid.org/0000-0002-0172-4524
Satoru Arai: http://orcid.org/0000-0003-3632-4392
Tatsuro Irimura: http://orcid.org/0000-0002-4709-3131
Shigaku Ikeda: http://orcid.org/0000-0002-7520-0707

CONFLICT OF INTEREST

The authors state no conflict of interest.

ACKNOWLEDGMENTS

We wish to thank Shinya Yamahira (Center for Medical Sciences of St. Luke's International University, Tokyo, Japan) for providing valuable advice on confocal image analysis. This work was supported by the Japan Society for the Promotion of Science (KAKENHI grant numbers JP19K23852 and JP20K07163) and the Japan Agency for Medical Research and Development (grant number JP19ae0101026).

AUTHOR CONTRIBUTIONS

Conceptualization: YMZ, KDN, TI; Data Curation: YMZ, RM; Formal Analysis: YMZ; Funding Acquisition: YMZ, KDN, TI; Investigation: YMZ, MN, NT; Methodology: YMZ, KDN; Project Administration: KDN; Resources: YMZ, MN; Supervision: KDN, NK, SA, TI, SI; Visualization: YMZ, KBIS; Writing – Original Draft Preparation: YMZ; Writing – Review and Editing: YMZ, KDN, KBIS, TI

Disclaimer

The sponsors had no role in the collection, analysis, and interpretation of data; in the writing of the report; or in the decision to submit the article for publication.

Yukari Manome-Zenke[1,2], *Kaori Denda-Nagai*[3,*], *Ryuichi Murakami*[4], *Miki Noji*[5],

Naoto Tsuneda[6], Katrin Beate Ishii-Schrade[5], Naoki Kanomata[6], Satoru Arai[1], Tatsuro Irimura[5] and Shigaku Ikeda[2]

[1]Department of Dermatology, St. Luke's International Hospital, Tokyo, Japan; [2]Department of Dermatology and Allergology, Graduate School of Medicine, Juntendo University, Tokyo, Japan; [3]Intractable Disease Research Center, Graduate School of Medicine, Juntendo University, Tokyo, Japan; [4]Laboratory of Immunology and Microbiology, Graduate School of Pharmaceutical Sciences, The University of Tokyo, Tokyo, Japan; [5]Division of Glycobiologics, JARIHES, Juntendo University, Tokyo, Japan; and [6]Department of Pathology, St. Luke's International Hospital, Tokyo, Japan
*Corresponding author e-mail: k-denda@juntendo.ac.jp

SUPPLEMENTARY MATERIAL

Supplementary material is linked to the online version of the paper at https://doi.org/10.1016/j.jid.2023.03.1654

REFERENCES

Bourdely P, Anselmi G, Vaivode K, Ramos RN, Missolo-Koussou Y, Hidalgo S, et al. Transcriptional and functional analysis of CD1c$^+$ human dendritic cells identifies a CD163$^+$ subset priming CD8$^+$CD103$^+$ T cells. Immunity 2020;53:335–52.e8.

Brown CC, Gudjonson H, Pritykin Y, Deep D, Lavallée VP, Mendoza A, et al. Transcriptional basis of mouse and human dendritic cell heterogeneity. Cell 2019;179:846–63.e24.

Denda-Nagai K, Aida S, Saba K, Suzuki K, Moriyama S, Oo-Puthinan S, et al. Distribution and function of macrophage galactose-type C-type lectin 2 (MGL2/CD301b): efficient uptake and presentation of glycosylated antigens by dendritic cells. J Biol Chem 2010;285:19193–204.

Gao Y, Nish SA, Jiang R, Hou L, Licona-Limón P, Weinstein JS, et al. Control of T helper 2 responses by transcription factor IRF4-dependent dendritic cells. Immunity 2013;39:722–32.

Guttman-Yassky E, Lowes MA, Fuentes-Duculan J, Whynot J, Novitskaya I, Cardinale I, et al. Major differences in inflammatory dendritic cells and their products distinguish atopic dermatitis from psoriasis. J Allergy Clin Immunol 2007;119:1210–7.

Heger L, Balk S, Lühr JJ, Heidkamp GF, Lehmann CHK, Hatscher L, et al. CLEC10A is a specific marker for human CD1c$^+$ dendritic cells and enhances their toll-like receptor 7/8-induced cytokine secretion. Front Immunol 2018;9:744.

Kanemaru K, Noguchi E, Tahara-Hanaoka S, Mizuno S, Tateno H, Denda-Nagai K, et al. Clec10a regulates mite-induced dermatitis [published correction appears in Sci Immunol 2020;5:eabg0688]. Sci Immunol 2019;4:eaax6908.

Kashem SW, Haniffa M, Kaplan DH. Antigen-presenting cells in the skin. Annu Rev Immunol 2017;35:469–99.

Kataoka Y. Thymus and activation-regulated chemokine as a clinical biomarker in atopic dermatitis. J Dermatol 2014;41:221–9.

Kim TG, Kim SH, Park J, Choi W, Sohn M, Na HY, et al. Skin-specific CD301b$^+$ dermal dendritic cells drive IL-17-mediated psoriasis-like immune response in mice. J Invest Dermatol 2018;138:844–53.

Kumamoto Y, Denda-Nagai K, Aida S, Higashi N, Irimura T. MGL2 Dermal dendritic cells are sufficient to initiate contact hypersensitivity in vivo. PLoS One 2009;4:e5619.

Kumamoto Y, Linehan M, Weinstein JS, Laidlaw BJ, Craft JE, Iwasaki A. CD301b$^+$ dermal dendritic cells drive T helper 2 cell-mediated immunity. Immunity 2013;39:733–43.

Kurashina R, Denda-Nagai K, Saba K, Hisai T, Hara H, Irimura T. Intestinal lamina propria macrophages upregulate interleukin-10 mRNA in response to signals from commensal bacteria recognized by MGL1/CD301a. Glycobiology 2021;31:827–37.

Murakami R, Denda-Nagai K, Hashimoto S, Nagai S, Hattori M, Irimura T. A unique dermal dendritic cell subset that skews the immune response toward Th2. PLoS One 2013;8:e73270.

Nakamizo S, Dutertre CA, Khalilnezhad A, Zhang XM, Lim S, Lum J, et al. Single-cell analysis of human skin identifies CD14+ type 3 dendritic cells co-producing IL1B and IL23A in psoriasis. J Exp Med 2021;218:e20202345.

Nattkemper LA, Tey HL, Valdes-Rodriguez R, Lee H, Mollanazar NK, Albornoz C, et al. The genetics of chronic itch: gene expression in the skin of patients with atopic dermatitis and psoriasis with severe itch. J Invest Dermatol 2018;138:1311–7.

Polak ME, Thirdborough SM, Ung CY, Elliott T, Healy E, Freeman TC, et al. Distinct molecular signature of human skin Langerhans cells denotes critical differences in cutaneous dendritic cell immune regulation. J Invest Dermatol 2014;134:695–703.

Purzycka-Bohdan D, Nedoszytko B, Zabłotna M, Gleń J, Szczerkowska-Dobosz A, Nowicki RJ. Chemokine profile in psoriasis patients in correlation with disease severity and pruritus. Int J Mol Sci 2022;23:13330.

Saeki H, Tamaki K. Thymus and activation regulated chemokine (TARC)/CCL17 and skin diseases. J Dermatol Sci 2006;43:75–84.

Tanei R, Hasegawa Y. Immunohistopathological analysis of immunoglobulin E-positive epidermal dendritic cells with house dust mite antigens in naturally occurring skin lesions of adult and elderly patients with atopic dermatitis. Dermatopathology (Basel) 2021;8:426–41.

Tanei R, Hasegawa Y. Immunological pathomechanisms of spongiotic dermatitis in skin lesions of atopic dermatitis. Int J Mol Sci 2022;23:6682.

Stage of Keratinocyte Differentiation Is a Key Determinant of Viral Susceptibility in Human Skin

Journal of Investigative Dermatology (2023) **143,** 1838–1841; doi:10.1016/j.jid.2023.03.1656

TO THE EDITOR

The human epidermis is composed of four visually distinct layers: the stratum basale, stratum spinosum, stratum granulosum, and stratum corneum, which result from a complex differentiation process. This study utilized in vitro viral infection assays with cultured human keratinocytes (KCs), bioinformatic analysis of epidermal single-cell RNA-sequencing datasets, and histopathologic assessment of human viral skin infections (herpes simplex virus [HSV] and varicella-zoster virus [VZV]) to address whether specific KC layers and/or stages of differentiation are more susceptible to viral infection and/or spread.

Human KCs (N/TERT2G) were infected with fluorescently-tagged HSV-1 at various stages of differentiation (Figure 1a). Cells were exposed to the virus for 3 days and then analyzed by

Abbreviations: HSV, herpes simplex virus; KC, keratinocyte; VZV, varicella-zoster virus

Accepted manuscript published online 28 March 2023; corrected proof published online 27 April 2023

SUPPLEMENTARY RESULTS

Increased macrophage galactose-type C-type lectin mRNA expression in skin biopsies from patients with atopic dermatitis and psoriasis compared with that in healthy controls on the basis of analysis of publicly available gene expression data

In the GSE121212 dataset, macrophage galactose-type C-type lectin (*MGL*) mRNA expression was upregulated in atopic dermatitis (AD) compared with that in healthy controls (HCs) ($\log_2$ fold change [FC] = 2.29, $P = 1.27 \times 10^{-26}$, false discovery rate [FDR] = 1.64×10^{-24}) (Supplementary Figure S3a) and in psoriasis (Pso) compared with that in HCs ($\log_2$ FC = 1.40, $P = 3.21 \times 10^{-12}$, FDR = 1.75×10^{-11}) (Supplementary Figure S3b). In the E-MTAB-8149 dataset, *MGL* mRNA expression was upregulated in AD compared with that in HCs ($\log_2$ FC = 1.25, $P = 4.12 \times 10^{-51}$, FDR = 5.79×10^{-49}) (Supplementary Figure S3c) and in Pso compared with that in HCs ($\log_2$ FC = 0.74, $P = 3.95 \times 10^{-34}$, FDR = 3.62×10^{-33}) (Supplementary Figure S3d).

SUPPLEMENTARY MATERIALS AND METHODS

Patient information and tissue samples

We collected human skin tissue samples from patients diagnosed with Pso (n = 16), patients diagnosed with AD (n = 11), and HCs (*n* = 12) who visited the Department of Dermatology at St. Luke's International Hospital (Tokyo, Japan) during the period from March 2018 to October 2021. One specimen was taken per patient from the location with the most severe skin inflammation in the patient. All patients were asked to pause their skin medications for 1 week before the skin biopsy. For HC specimens, we obtained the residual sample from patients who visited our department for the resection of a noninflammatory benign skin tumor. Pediatric patients and patients with generalized pustular Pso were excluded from this study. Skin biopsies were taken, and peripheral blood was collected within a few days of the skin tissue sampling for the determination of serum TARC/CCL17 and total IgE levels. As a clinical severity score, Eczema Area and Severity Index of 0–72 for AD and Psoriasis Area and Severity Index of 0–72 for Pso were evaluated by a dermatologist.

Reagents

We previously established an anti-human MGL mAb (MLD-16) (Sano et al., 2007). We tested the applicability of MLD-16 on formalin-fixed paraffin-embedded tissue sections in comparison with a rabbit polyclonal antibody specific for MGL/CLEC10A (Atlas, Stockholm, Sweden) (Supplementary Figure S1) and examined the immunohistochemical localizations of MGL^+ cells using the polyclonal antibody. For TARC/CCL17, a rabbit polyclonal antibody (Abcam, Cambridge, United Kingdom) was used as the primary antibody. The Ventana Optiview Detection Kit (Roche Diagnostics, Basel, Switzerland) was used as the secondary reagent. For immunofluorescence, MLD-16 and antibodies specific for CD1a (polyclonal rabbit, Atlas), CD1c (clone M241, Absolute Antibody, Wilton, United Kingdom), CD14 (clone SC69-02, Novusbio, Centennial, CO), and CD68 (clone EPR20545, Abcam) were used. Goat anti-mouse IgG (H+L) antibody Alexa Flour 488 (Jackson Immuno Research, West Grove, PA) and goat anti-rabbit IgG (H+L) antibody Alexa Flour 594 (Thermo Fisher Scientific, Waltham, MA) were used as secondary reagents. Vectashield Vibrance Antifade Mounting Medium with DAPI (Funakoshi, Tokyo, Japan) was used for DAPI staining.

Immunohistochemistry

Skin samples were fixed in formalin, embedded in paraffin, and sectioned to 3 μm. Fixed sections were stained with MLD-16 monoclonal or anti-MGL/CLEC10A polyclonal antibodies and anti-TARC/CCL17 antibodies using an automatic staining machine (Ventana Benchmark Ultra, Roche Diagnostics). The number of MGL^+ cells and $TARC^+$ cells in different areas (five fields per slide) were determined. MGL^+ cells were quantified separately in the epidermis and dermis. The cell numbers per unit area (cells/mm^2) were counted manually using light microscopy (biological microscope BX53, Olympus, Tokyo, Japan) and analyzed using Fiji imaging software (Schindelin et al., 2012).

Immunofluorescence

Skin samples were frozen in Tissue-Tek O.C.T. compound (Sakura Finetek, Tokyo, Japan), and 4 μm thick sections were cut. The sections were fixed with cold methanol for 30 seconds and blocked with 3% BSA (Sigma-Aldrich, St. Louis, MO) in PBS (Nacalai Tesque, Kyoto, Japan) for 60 minutes at room temperature. For costaining with immune cell markers, the sections were incubated with MLD-16 mAb and antibodies specific for CD1a, CD1c, CD14, CD68, or TARC/CCL17 diluted in PBS containing 0.1 M calcium chloride (Nacalai Tesque) and 0.5M magnesium chloride (Nacalai Tesque) overnight at 4 C. After washing with PBS, the sections were incubated with secondary antibodies (anti-mouse IgG antibody Alexa Flour 488 and anti-rabbit IgG antibody Alexa Flour 594) for 30 minutes at room temperature in the dark. After washing with PBS, the sections were mounted with Vectashield Vibrance Antifade Mounting Medium, which contains DAPI as a nuclear stain. Stained sections were imaged, and pictures were taken by confocal microscopy (DMI6000b, Leica Microsystems, Wetzlar, Germany). The images were imported into Fiji image analysis software, and an area containing about 100 DAPI-stained cells was defined as one counting area. For AD and Pso specimens, areas comprising a lesion were selected. The number of $DAPI^+MGL^+$ and $DAPI^+MGL^+$ immune cell marker−positive cells per unit area was counted manually in three different areas per patient specimen. Specimens from three individuals were examined for each of the HC, AD, and Pso groups.

Measurement of serum TARC/CCL17 and serum total IgE levels

Serum levels of TARC/CCL17 and total IgE were measured as part of the routine clinical diagnostic laboratory tests conducted at St. Luke's International Hospital.

MGL mRNA gene expression analysis of publicly available data from patients with AD and Pso and HCs

Because the sample size of this study was relatively small, we sought to provide supportive evidence for increased *MGL* expression in AD and Pso on the mRNA level using publicly available RNA-

sequencing and microarray data. We scrutinized the Gene Expression Omnibus (https://www.ncbi.nlm.nih.gov/gds/) and the EBI ArrayExpress (https://www.ebi.ac.uk/arrayexpress/) databases for studies investigating differentially expressed genes in patients with AD and Pso and healthy volunteers. Selection criteria were (i) skin biopsy samples (ii) a large sample size, (iii) a comparable severity of AD and Pso (as judged by Severity Scoring of Atopic Dermatitis, Eczema Area and Severity Index, and Psoriasis Area and Severity Index scores) as in this study, (iv) a comparable age range as in this study, and (v) the availability of mRNA expression data on *MGL* and *TARC/CCL17*.

Two datasets—Gene Expression Omnibus GSE121212 (n = 142) (https://www.ncbi.nlm.nih.gov/geo/query/acc.cgi?acc=GSE121212) and EBI ArrayExpress E-MTAB-8149 (n = 402) (www.ebi.ac.uk/arrayexpress/experiments/E-MTAB-8149/)—fulfilled these criteria. Next, we confirmed that genes that had been previously reported as commonly upregulated in AD and Pso (Ghosh et al., 2015; Tian et al., 2012), such as *KYNU*, *PI3*, and *IL17A*, were also upregulated in GSE121212 and E-MTAB-8149. On the basis of this, we judged that the GSE121212 and E-MTAB-8149 datasets were sufficiently suitable for our purpose of gaining supportive evidence from publicly available data. Read count data of GSE121212 were downloaded from Gene Expression Omnibus, and differentially expressed genes in AD compared with those in HC and in Pso compared with those in HC were analyzed using edgeR (version 3.28.1) (McCarthy et al., 2012; Robinson et al., 2010) at criteria in which the FDR was <0.05, and the absolute $\log_2$ FC of gene expression was >0.5.

CEL files of E-MTAB-8149 were downloaded from EBI ArrayExpress and processed using oligo (version 1.58.0) (Carvalho and Irizarry, 2010). Annotation was added using pd.hugene.2.1.st (version 3.14.1) (Carvalho, 2015). Differentially expressed genes in AD compared with those in HC and in Pso compared with those in HC were analyzed using limma (version 3.50.3) (Ritchie et al., 2015) at criteria in which the FDR was <0.05, and the absolute $\log_2$ FC of gene expression was >0.5. R (version 4.1 or 3.6) was used for the analysis.

Statistical analysis

The Kruskal–Wallis test was used to analyze differences between MGL^+ cell numbers in HC, AD, and Pso specimens. Spearman's rank correlation was used to analyze the correlation between the number of MGL^+ cells in the skin and serum TARC/CCL17, serum total IgE, and $TARC^+$ cells in the skin. A $P < 0.05$ was considered statistically significant. Except where stated otherwise, all statistical analyses were performed with the Statistical Package for Social Sciences software, version 18.0 (SPSS, Chicago, IL).

SUPPLEMENTARY REFERENCES

Carvalho B. Platform Design Info for Affymetrix HuGene-2_1-st. https://bioconductor.org/packages/release/data/annotation/html/pd.hugene.2.1.st.html; 2015. (accessed May 1, 2022).

Carvalho BS, Irizarry RA. A framework for oligonucleotide microarray preprocessing. Bioinformatics 2010;26:2363–7.

Ghosh D, Ding L, Sivaprasad U, Geh E, Biagini Myers J, Bernstein JA, et al. Multiple transcriptome data analysis reveals biologically relevant atopic dermatitis signature genes and pathways. PLoS One 2015;10:e0144316.

McCarthy DJ, Chen Y, Smyth GK. Differential expression analysis of multifactor RNA-Seq experiments with respect to biological variation. Nucleic Acids Res 2012;40:4288–97.

Ritchie ME, Phipson B, Wu D, Hu Y, Law CW, Shi W, et al. limma powers differential expression analyses for RNA-sequencing and microarray studies. Nucleic Acids Res 2015;43:e47.

Robinson MD, McCarthy DJ, Smyth GK. edgeR: a Bioconductor package for differential expression analysis of digital gene expression data. Bioinformatics 2010;26:139–40.

Sano Y, Usami K, Izawa R, Denda-Nagai K, Higashi N, Kimura T, et al. Properties of blocking and non-blocking monoclonal antibodies specific for human macrophage galactose-type C-type lectin (MGL/ClecSF10A/CD301). J Biochem 2007;141:127–36.

Schindelin J, Arganda-Carreras I, Frise E, Kaynig V, Longair M, Pietzsch T, et al. Fiji: an open-source platform for biological-image analysis. Nat Methods 2012;9:676–82.

Tian S, Krueger JG, Li K, Jabbari A, Brodmerkel C, Lowes MA, et al. Meta-analysis derived (MAD) transcriptome of psoriasis defines the "core" pathogenesis of disease. PLoS One 2012;7:e44274.

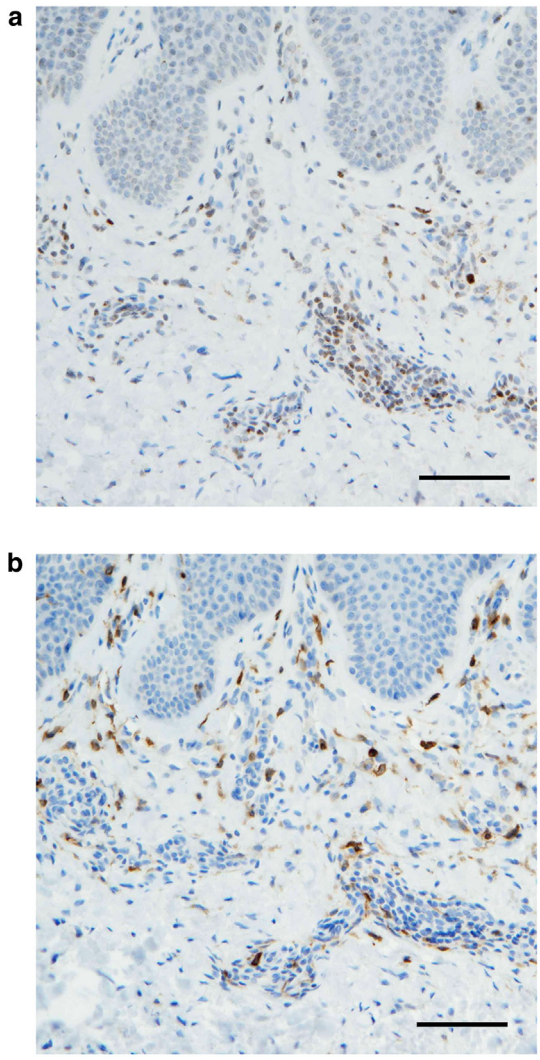

Supplementary Figure S1. Comparison of the staining intensity between a mAb (MLD-16) and a polyclonal antibody against human MGL in the dermis of a patient with psoriasis. (**a**) mAb (MLD-16). (**b**) Polyclonal antibody. Bar = 100 μm. The polyclonal antibody staining was stronger; therefore, we used the polyclonal antibody for the staining shown in Figure 1a–c. MGL, macrophage galactose-type C-type lectin.

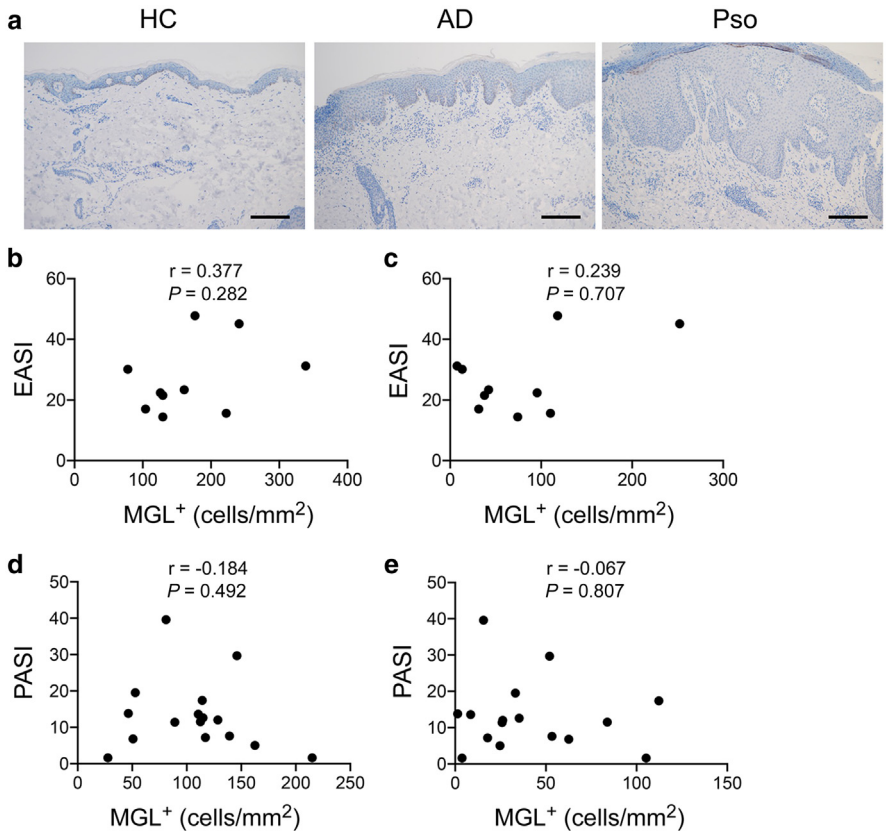

Supplementary Figure S2. Distribution and density of MGL$^+$ cells in human skin. (**a**) Control antibody staining in HCs and in patients with AD and Pso. Bar = 200 μm. (**b, c**) Correlation between the density of MGL$^+$ cells and EASI. (**b**) AD dermis; (**c**) AD epidermis. (**d, e**) Correlation between the density of MGL$^+$ cells and PASI. (**d**) Pso dermis; (**e**) Pso epidermis. Spearman's rank correlation r is shown. AD, atopic dermatitis; EASI, Eczema Area and Severity Index; HC, healthy control; MGL, macrophage galactose-type C-type lectin; PASI, Psoriasis Area and Severity Index; Pso, psoriasis.

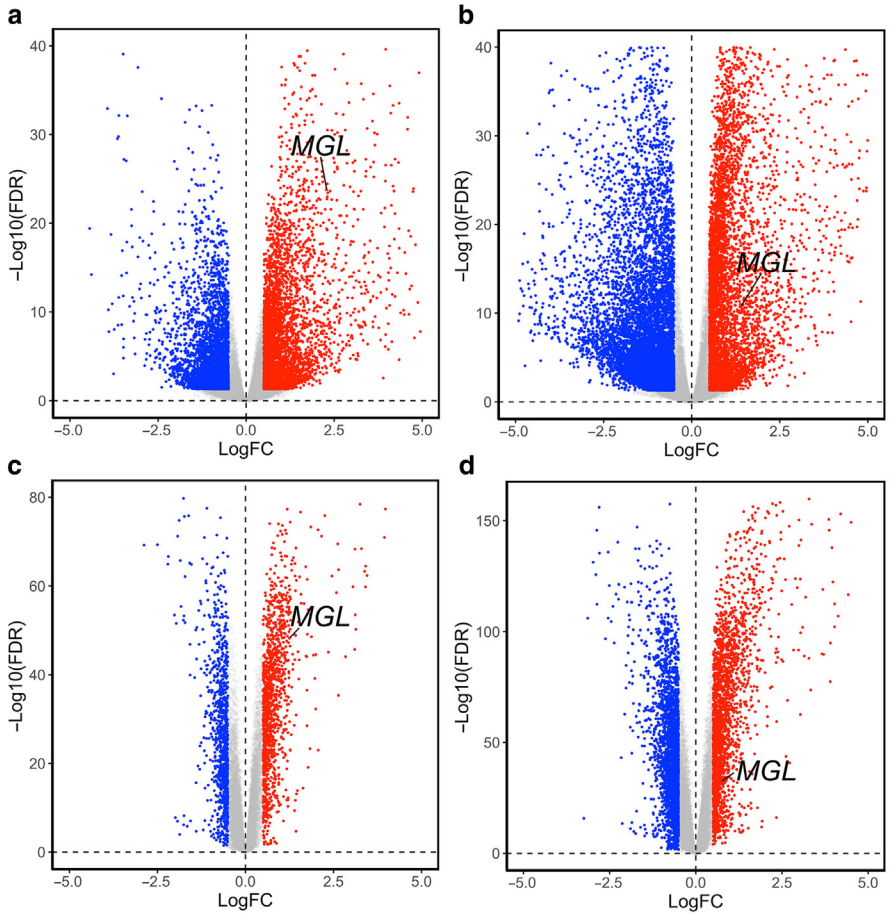

Supplementary Figure S3. Volcano plots of differentially expressed genes in skin biopsy specimens from patients with AD and Pso compared with those from HCs. Two publicly available datasets were analyzed: (**a**) GEO GSE121212 (AD vs. HC) and (**b**) GEO GSE121212 (Pso vs. HC) and (**c**) ArrayExpress E-MTAB-8149 (AD vs. HC) and (**d**) ArrayExpress E-MTAB-8149 (Pso vs. HC). The position of *MGL* is indicated. Blue: downregulated genes. Red: upregulated genes.
AD, atopic dermatitis; FC, fold change; FDR, false discovery rate; GEO, Gene Expression Omnibus; HC, healthy control; MGL, macrophage
galactose-type C-type lectin; Pso, psoriasis.

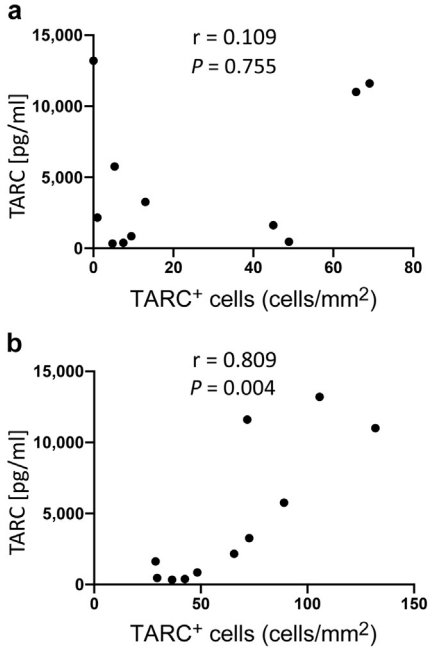

Supplementary Figure S4. Correlation between serum TARC levels and the numbers of TARC$^+$ cells in atopic dermatitis skin. Each dot represents one patient. (**a**) Epidermis. (**b**) Dermis. r denotes Spearman's rank correlation coefficient.

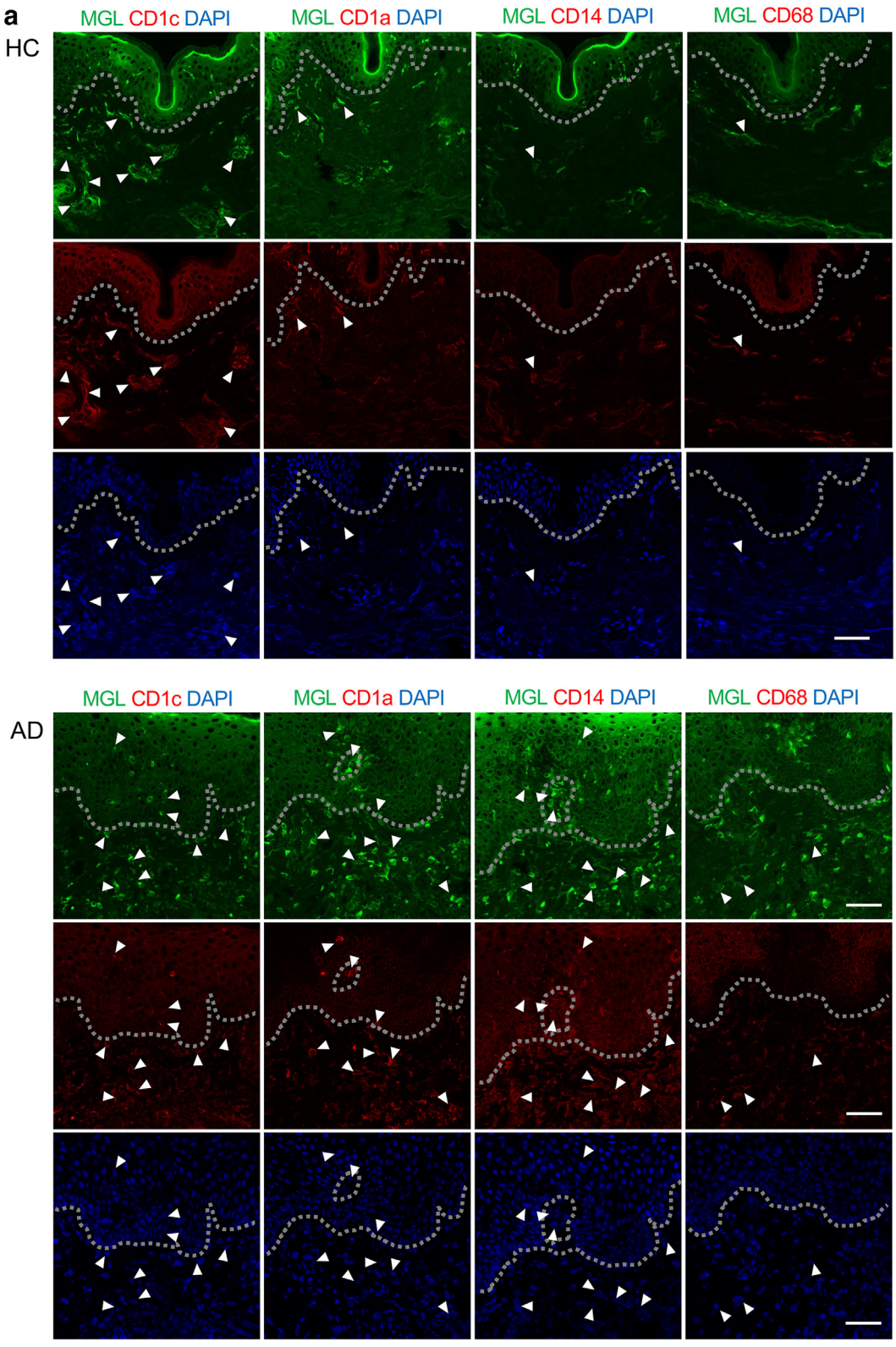

Supplementary Figure S5. Phenotypes of MGL$^+$ cells in HC and AD and Pso skin. (**a**) Phenotypes of MGL$^+$ cells in HC and AD skin. This figure shows the single-channel images for the merged images shown in Figure 2a. Skin biopsy specimens from HCs and patients with AD were costained with a mAb specific for MGL and antibodies specific for the innate immune cell markers CD1c, CD1a, CD14, and CD68. Specimens from three patients each were investigated, and representative images are shown. Arrowheads indicate double-stained cells. A thin, dotted line indicates the border between the dermis and the epidermis. Bar = 50 μm. **(b)** Phenotypes of MGL$^+$ cells in HCs and Pso skin. This figure shows the single-channel images for the merged images shown in Figure 2b. Skin biopsy specimens from HC and patients with Pso were costained with a mAb specific for MGL and antibodies specific for the innate immune cell markers CD1c, CD1a, CD14, and CD68. Specimens from three patients each were investigated, and representative images are shown. Arrowheads indicate double-stained cells. A thin, dotted line indicates the border between the dermis and the epidermis. Bar = 100 μm. **(c)** Phenotypes of

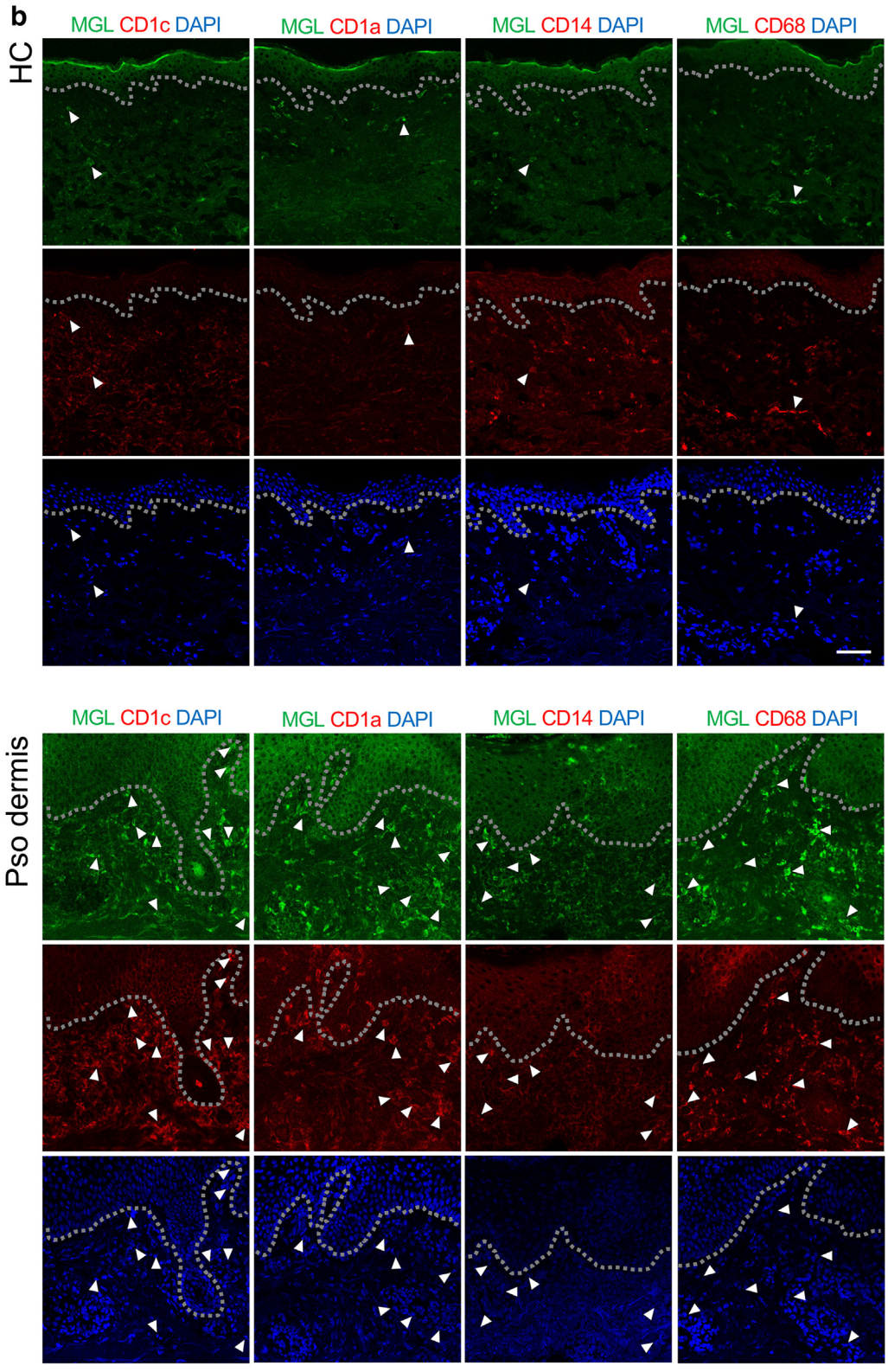

Supplementary Figure S5. Continued.

MGL^+ cells in HC, AD, and Pso skin. This figure shows the single-channel images for the merged images shown in Figure 2c. Biopsy specimens from HCs and patients with AD and Pso were costained with a mAb specific for MGL and a polyclonal antibody specific for TARC/CCL17 and investigated by immunofluorescence. Specimens from three patients each were investigated, and representative images are shown. Arrowheads indicate double-stained cells. A thin, dotted line indicates the border between the dermis and the epidermis. Bar = 50 μm. AD, atopic dermatitis; HC, healthy control; MGL, macrophage galactose-type C-type lectin; Pso, psoriasis.

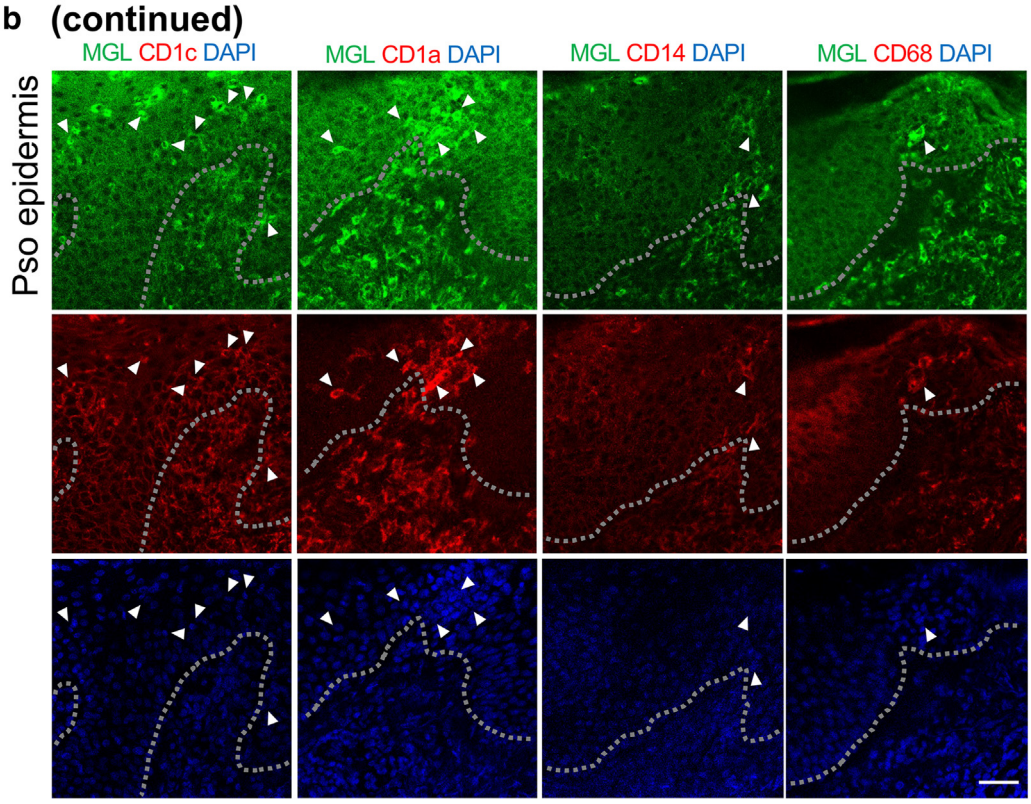

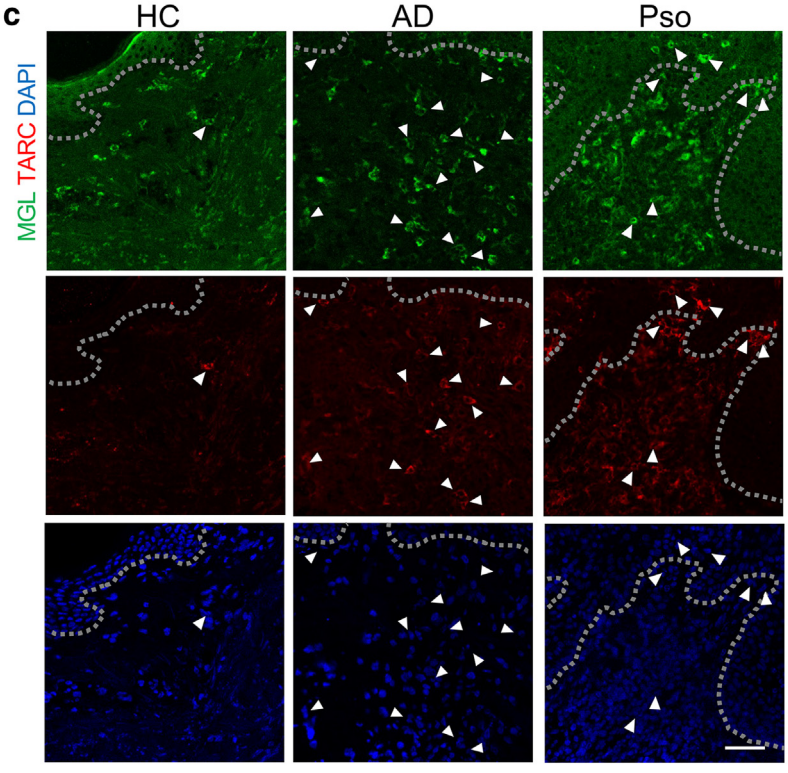

Supplementary Figure S5. Continued.

a

Immune cell marker	HC (%)	AD (%)	Pso (%)
CD1a	47.2 (13.0–63.1)	46.0 (22.5–58.6)	53.8 (52.8–78.8)
CD1c	71.6 (68.2–84.6)	79.7 (74.6–89.4)	82.9 (80.7–90.9)
CD14	50.0 (39.4–66.7)	85.3 (83.3–86.2)**	83.6 (80.6–93.1)*
CD68	42.9 (37.8–55.8)	55.4 (46.5–68.7)	50.9 (47.5–58.3)
TARC	9.1 (0.0–11.1)	65.7 (51.1–68.9)**	28.6 (14.0–75.0)*

b

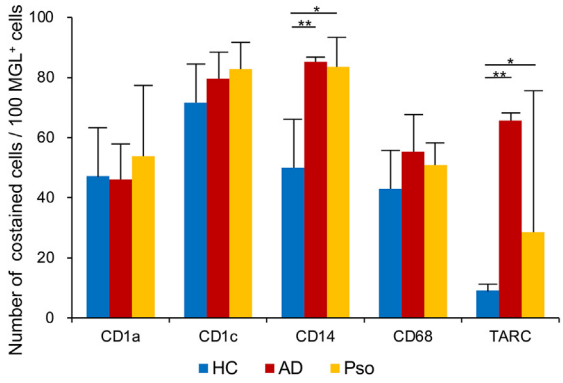

Supplementary Figure S6. Number of costained cells for each immune cell marker. (**a, b**) Semiquantitative data from the double-staining immunohistochemistry experiment shown in Figure 2. Skin biopsy specimens from HCs and patients with AD and Pso were stained with antibodies specific to MGL, CD1a, CD1c, CD14, CD68, and TARC. The number of cells costained with anti-MGL antibody and each of the other immune cell markers was counted. The data represents the median (interquartile range = 25−75%) of three counting areas in one specimen from three patients each. Error bars show a 75% interquartile range. Analysis was performed with Kruskal−Wallis test: $*P < 0.01$ and $**P < 0.001$. AD, atopic dermatitis; HC, healthy control; MGL, macrophage galactose-type C-type lectin; Pso, psoriasis.

Supplementary Table S1. Subject Characteristics

No	Age/ Sex	Diagnosis	Serum Total IgE (IU/ml)	Serum TARC (pg/ml)	TARC$^+$Cells in Epidermis (Cells/mm^2)	TARC$^+$Cells in Dermis (Cells/mm^2)	MGL$^+$Cells in Epidermis (Cells/mm^2)	MGL$^+$Cells in Dermis (Cells/mm^2)	PASI or EASI
1	40/M	HC	—	—	—	—	0.0	35.1	—
2	33/F	HC	—	—	—	—	14.5	58.1	—
3	59/F	HC	—	—	—	—	3.4	32.5	—
4	33/M	HC	—	—	—	—	0.0	24.9	—
5	69/M	HC	—	—	—	—	1.9	25.4	—
6	31/F	HC	—	—	—	—	0.0	24.8	—
7	71/F	HC	—	—	—	—	0.0	26.2	—
8	60/M	HC	—	—	—	—	0.0	27.2	—
9	28/F	HC	—	—	—	—	0.0	26.4	—
10	51/M	HC	—	—	—	—	0.0	24.3	—
11	62/F	HC	—	—	—	—	2.8	40.9	—
12	43/M	HC	—	—	—	—	0.0	22.3	—
13	51/F	AD	>25,000	13,200	0.0	105.7	7.5	338.7	31.2
14	54/M	AD	>25,000	11,000	65.7	131.9	252.2	241.2	45.1
15	71/M	AD	2,800	3,260	13.0	72.7	110.3	222.4	15.6
16	41/M	AD	3,300	11,600	69.1	71.8	118.0	176.6	47.8
17	48/F	AD		450	48.9	29.5	59.0	168.4	2.4
18	46/M	AD	820	2,160	1.0	65.6	42.2	160.8	23.4
19	44/M	AD	770	332	4.8	36.5	74.2	129.5	14.4
20	47/F	AD	6,900	848	9.5	48.4	37.7	129.5	21.5
21	85/M	AD	820	5,750	5.3	89.0	95.6	125.9	22.4
22	44/M	AD	180	1,620	45.0	28.8	31.4	104.2	17.0
23	36/M	AD	—	382	7.5	42.5	13.3	78.1	30.1
24	52/F	Pso	—	—	2.4	37.7	52.0	146.0	29.7
25	31/M	Pso	—	—	0	55.3	25.9	89.1	11.4
26	62/M	Pso	—	—	7.4	23.0	112.3	114.3	17.4
27	57/M	Pso	—	—	4.2	126.7	35.3	114.9	12.6
28	41/M	Pso	—	—	3.8	14.5	15.6	81.0	39.6
29	41/M	Pso	—	—	2.5	20.9	33.2	52.9	19.5
30	27/F	Pso	—	—	6.2	43.2	62.6	50.8	6.8
31	77/M	Pso	—	—	13.3	124.4	83.9	112.5	11.5
32	35/M	Pso	—	—	2.3	57.3	105.3	215.0	1.6
33	30/F	Pso	—	—	0.0	7.9	1.4	46.4	13.8
34	67/M	Pso	—	—	1.6	34.3	8.5	110.6	13.6
35	43/F	Pso	—	—	0.0	34.9	3.8	27.7	1.6
36	62/F	Pso	—	—	7.5	74.9	53.4	139.3	7.6
37	58/F	Pso	—	—	2.8	75.7	17.9	117.1	7.2
38	74/F	Pso	—	—	3.4	88.5	24.7	162.6	5.0
39	47/F	Pso	—	—	9.7	57.8	26.2	128.6	12.0

Abbreviations: AD, atopic dermatitis; EASI, Eczema Area and Severity Index; F, female; HC, healthy control; M, male; PASI, Psoriasis Area and Severity Index; Pso, psoriasis.

A total of 39 patients—AD (n = 11), Pso (n = 16), and HC (n = 12)—were included in the analysis. The male:female ratios were 2:1 in AD, 1:1 in Pso, and 1:1 in HC, and the median age in each group was 49.5 years (interquartile range = 39.5–62.0) in AD, 47.0 years (interquartile range = 44.0–52.5) in Pso, and 47.0 years (interquartile range = 33.0–60.5) in HC. The median EASI and PASI scores were 22.4 (interquartile range = 16.3–30.65) and 11.8 (interquartile range = 7.1–14.7), respectively.